10.1109/ULTSYM.2012.0510

Characterizing Ultrasound-controlled Drug Release by High-speed Fluorescence Imaging

Ying Luan[1], Erik Gelderblom[2] , Guillaume Lajoinie[2], Ilya Skachkov[1], Heleen Dewitte[3], Bart Geers[3], Ine Lentacker[3], Ton van der Steen[1], Michel Versluis[2] and Nico de Jong[1]
[1]Erasmus Medical Center, Rotterdam, the Netherlands
[2]University of Twente, Enschede, the Netherlands
[3]University of Ghent, Gent, Belgium

***Abstract* — Ultrasound contrast agents (UCAs) microbubbles (MBs) can be preloaded with a therapeutic agents to achieve high efficiency for US-triggered drug delivery. Here we use fluorescence labeling as a substitute for theraputic drug, and use ultra high-speed fluorescence imaging for time-resolved observation of the drug release. Two configurations of drug delivery vehicles were investigated - I) lipid-shelled (unloaded) MBs and II) liposome-loaded (loaded) MBs. Different release phenomena were observed. The dynamics of release was found to be strongly dependent on ultrasonic parameters and on the MB's shell properties. MBs shrinkage following US exposure was analyzed and it indicated close correlation with the fluorescence release. This study provides valuable insights into the drug release mechanisms for ultrasound-controlled drug delivery.**

Keywords – controlled release, fluorescence labeling, high-speed fluorescence imaging, release dynamics, drug delivery

I. INTRODUCTION

Ultrasound contrast agents (UCAs) microbubbles (MBs) are under extensive investigations as a drug delivery vehicle in applications of bubble enhanced drug delivery. Besides co-administration of drug molecules and MBs, drug-loaded MBs are developed to increase drug delivery efficiency and safety. MBs can be preloaded with drugs in several configurations: a) enclose the drugs within the core of MBs, e.g. by dissolving them in an oil layer; b) incorporate the drugs in the shell; and c) attach the drugs to the shell [1]. In a further step, a high payload can be achieved by attaching microcapsules to the MBs shell. A newly designed liposome-loaded MBs was developed by conjugating liposomes to MBs surface through covalent thiol-maleimide links [2]. Since liposomes are membrane-enclosed vesicles composed of a lipid bilayer shell surrounding an aqueous core, it can carry both lipophilic and hydrophilic drugs efficiently [3].

An essential step in the process of ultrasound-triggered drug delivery is the release of the therapeutic agent from the bubble surface. The nature of the release relies heavily on the intrinsic physical driving mechanisms of the release, and it also strongly depend on the applied ultrasound parameters, such as acoustical pressure, frequency and the number of cycles[4].

Here we present a parametric study into the controlled release from drug-loaded MBs of two drug loading configurations: lipid-shelled MBs with drugs incorporated in the shell, and liposome-loaded MBs with drugs encapsulated within liposomes. We use fluorescence labeling to resolve the drug molecules or liposomes in a small size scale, from several nanometers to 200 nm, and using a continuous wave (CW) laser as the excitation illumination for the fluorescence microscopy. A high-speed camera running at 100,000 fps is applied to visualize the drug release and transport dynamics triggered by ultrasound, at a fixed insonation frequency of 1MHz for a peak-negative pressure varying from 20 to 100 kPa, and a pulse duration of 10 to 1000 cycles.

The goal of this study is to quantify the dynamics of drug release under various ultrasound settings, and to investigate the release mechanisms for different drug loading configurations.

II. MATERIALS AND METHODS

A. Microbubbles

Three fluorescently-labeled MBs samples were prepared to represent drug-loaded MBs of different configurations. Sample A contains lipid-shelled MBs with a DiI-labeled bubble shell, while sample B consists of liposome-loaded (loaded) MBs with DiI-labeled liposome shell. Sample A was designed to visualize the release of drug molecules from the MBs shell, while sample B is devised to study the release of liposomes. Sample C is a control system for sample B, consisting of loaded bubbles with encapsulated fluorescent dextran.

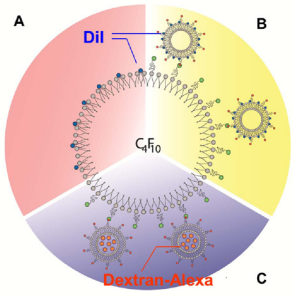

Figure 1. Schematic representation of the two configurations of bubble systems.

B. Microbubble formulations

MBs were prepared by mixing 1,2-dipalmitoyl-sn-glycero-3-phosphocholine (DPPC) (Lipoid, Ludwigshafen, Germany) and either 1,2-distearoyl-sn-glycero-3-phosphoethanolamine-N-[PDP(polyethylene glycol)-2000] (DSPE-PEG-SPDP) for functionalized bubbles or 1,2-distearoyl-sn-glycero-3-phosphoethanolamine-N-[methoxy(polyethylene glycol)-2000 (DSPEPEG)(both Avanti polar lipids, Alabaster, AL) for non-functionalized bubbles in a molar ratio of 65:35 in chloroform. For fluorescent labeling of the MBs membrane, the lipophilic dye DiI (Sigma-aldrich, Bornem, Belgium) was added to the

lipid mixture. After chloroform evaporation, the lipid film was dissolved in a 1:2:7 glycerine-propyleneglycol-H_2O mixture to obtain a clear solution with a final lipid concentration of 4×10^{-4} mmol/mL. This lipid solution was aliquotted in 2.5 mL chromatography vials of which the headspace was filled with perfluorobutane gas (F2 chemicals, Preston, UK). Finally, bubbles were obtained by high speed shaking of the chromatography vial in a Capmix™ device (3 M-ESPE, Diegem, Belgium) for 15 s.

Maleimide-functionalized liposomes were prepared by mixing DPPC, 1,2-distearoyl-snglycero-3-phosphoethanolamine-N-[maleimide(polyethylene glycol)-2000] (ammonium salt) (DSPE-PEG maleimide) (Laysan Bio Inc, Arab, AL), cholesterol and DiI, all dissolved in chloroform in a round-bottom flask at a 49:15:35:1 molar ratio and a final lipid concentration of 16 mg/mL lipids. The chloroform was evaporated and the remaining lipid film was hydrated with distilled water. The liposomes were sized by extrusion through a 200nm polycarbonate filter using a mini-extruder at 60°C (Avanti Polar Lipids, Alabaster, AL).

MBs were covalently loaded with maleimide-functionalized liposomes by adding 100 µL of the liposome dispersion to 900 µL of the bubble lipid mixture in a 2.5mL chromatography vial. After filling the headspace with perfluorobutane gas, the vial was shaken for 15 s in a CapMix™ device. This results in the formation of liposome-loaded MBs. Similarly, bubbles could be covalently loaded with Alexa Fluor® 546 C5 Maleimide (Molecular Probes®, Invitrogen, Merelbeke, Belgium) by adding an aliquot of a 1 mg/mL solution of this dye to the bubble lipid mixture in a chromatography vial, filling the headspace with perfluorobutane gas followed by high-speed shaking of the vial in a CapMix™ device for 15 s.

C. *High-speed fluorescence imaging setup*

The Opticell™ containing the MBs was placed in a water bath, located underneath an upright fluorescence microscope setup, depicted in Figure 2. The microscope was equipped with a 40× water-immersion objective (NA = 0.8; Olympus, The Netherlands). To achieve a high fluorescence signal, a continuous wave laser (5 W@532 nm; Cohlibri; Lightline, Germany) was employed for fluorescence excitation of the fluorescent label. The laser light was gated using an acousto-optic modulator (AOM) (AOTF.nC-VIS; AA Optoelectronic, France) to generate a single pulse with the duration of 6 ms to minimize heating of the sample. Bright field illumination was produced by a halogen light source (KL1500LCD, Schott, Germany). The intensity was adjusted to a level that allowed for monitoring of the bubble position during the high-speed fluorescence recordings.

High-speed fluorescence images of the liposome-loaded MBs were recorded with high-speed CMOS camera (SA-1.1; Photron Ltd,UK), operating at 100 kfps (320×160 pixels), starting 1 ms prior to ultrasound excitation for a duration of 6 ms (600 frames). The microscope was fitted with an 80/20 beamsplitter to allow for simultaneous video rate bright field recordings with a larger field of view at 15 fps using a highly sensitive CCD camera (LM165M; Lumenera Corporation, Canada). Bright field recordings were started one second before ultrasound excitation for a duration of 10 seconds to monitor the bubble displacement and eventually bubble shrinkage.

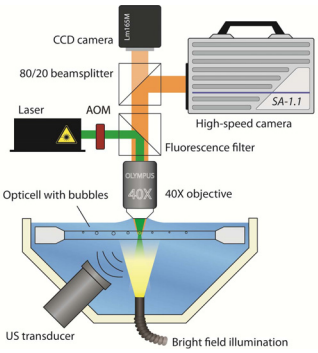

Figure 2. Schematic representation of the experimental setup.

MBs with diameters around 6 µm were investigated. 152 MBs of sample A and 193 MBs of sample B were divided into 15 groups each, with different ultrasound settings applied. The MBs were insonified by a single, sine-wave ultrasound pulse with a duration of 10, 100 or 1000 cycles at an ultrasound frequency of 1.0 MHz at five peak-negative pressures (20-100 kPa, 20 kPa step size) using a focused, single element transducer (C302; Panametrics, USA). The pressures generated by the transducer were calibrated with a 2 mm PVDF needle hydrophone (Precision Acoustics, UK). The shrinkage of 92 MBs of sample C during and after insonifications were measured. The cycles applied are 10, 50, 100, 200 and 500 cycles.

III. RESULTS

A. *Release Dynamics*

Three types of release dynamics from unloaded and loaded MBs were observed. The first type is the movement of fluorescent material over the bubble surface, and the movements were typically non-uniform and appeared random and chaotic. The lipids are shown to be “rearranged” or “build up” after the ultrasound excitation. These phenomena either occur independently as the initiation of shell material displacement, or are accompanied by the two types of release described subsequently. The second type can be described as the release of vesicles with a size on the order of several hundreds of nanometers that can be resolved by the optical system. The third type of release can be described as the release of a bulk of particles which are too small to be resolved individually, consequently observed as a “cloud” emerging from the MBs surface. This type of release takes place on a much shorter timescale, appearing as the instantaneous release of a large part of the fluorescent shell material, being expelled radially outwards. Figure 3 shows typical examples of the three types of release: rearrangement (R), vesicle release (V) and cloud release (C). Release events were counted for both unloaded and loaded bubbles, and the percentage of events in each group was plotted in Figure 4.

Drug release from the bubble surface was observed at acoustic pressures as low as 20 kPa for a pulse length of 100 cycles. In general, for both unloaded bubbles and loaded bubbles, with increasing pulse length and acoustic pressure, the release events increase correspondingly. Besides ultrasound

settings, drug loading configurations also greatly influence the release dynamics. The unloaded bubbles clearly show a lower threshold for release: applying 10 cycles mainly the unloaded bubbles showed release. For 1000 cycles both groups showed release even at an acoustic pressure as low as 20 kPa. Among all ultrasound settings, the percentage of loaded bubbles showing rearrangement of shell material is 420% higher than for unloaded bubbles, for vesicle release it is 80% higher, while for cloud release it is 46% lower.

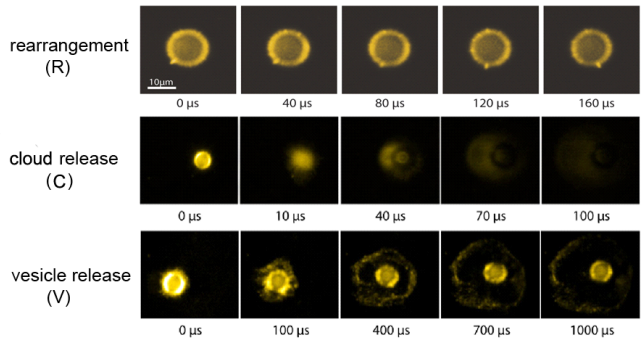

Figure 3. Three types of release dynamics for fluorescently labeled microbubles.

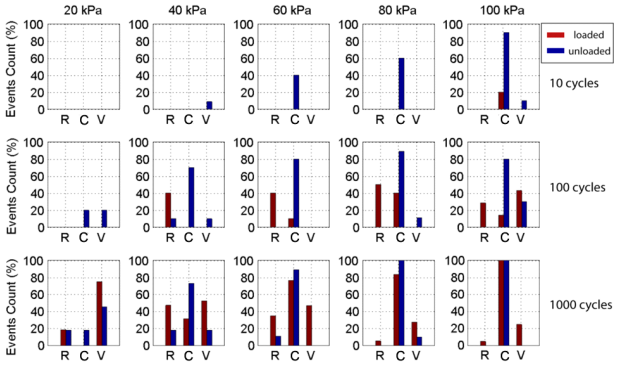

Figure 4. Events of release as functions of ultrasound parameters for unloaded and loaded MBs.

B. *Release distance/speed*

To evaluate the length scale and time scale on which the release occurs, the front of the released particles/cloud can be traced and the distance from the bubble interface was plotted as a function of time. Figure 5 shows an example of individual MBs insonified at a pressure of 100 kPa, for a series of cycles. For 10 cycles and 50 cycles, the release continues for 20 to 30 μs after ultrasound was turned off. However, for 100 cycles and 200 cycles, shell material stops to spread after the ultrasound is turned off. This could be due to the decreasing of the velocity of the released material with increasing of the transported distance. Longer pulses transport the material further from the microbubble, leading to a quicker stop after ultrasound has been turned off. The release speed derived from the data is on the order of 0.1 m/s.

C. *Acoustic dissolution*

Acoustically driven bubble dissolution was derived for sample C when insonified at a series of acoustic pressures (Figure 6) and cycles (Figure 7). MBs dissolution is

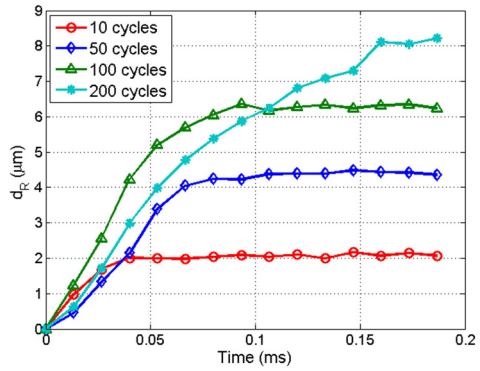

Figure 5. Release distance as a function of time at 100 kPa with different pulse lengths.

characterized by the normalized change in radius $\Delta R/R_0$, where ΔR is the bubble shrinkage immediately after insonification and R_0 is the initial radius of MBs. At each single pressure, the bubble shrinkage is diverted for individual MBs of different sizes. However, with increasing pressure, a clear increase of bubble dissolution can be observed. On the other hand, we found no clear dependency of the magnitude of the acoustic dissolution on the number of acoustic cycles.

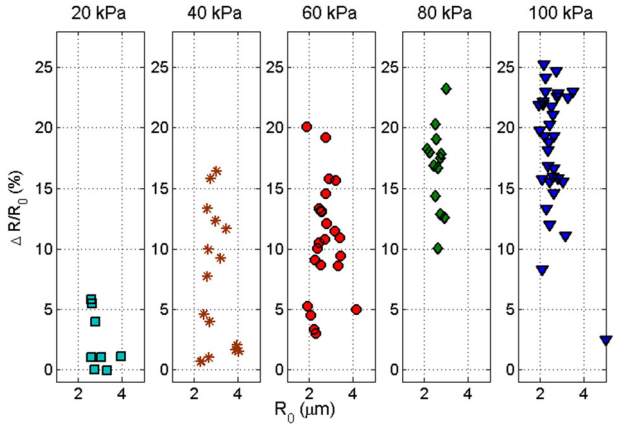

Figure 6. Acoustic dissolution as a function of applied acoustic pressure.

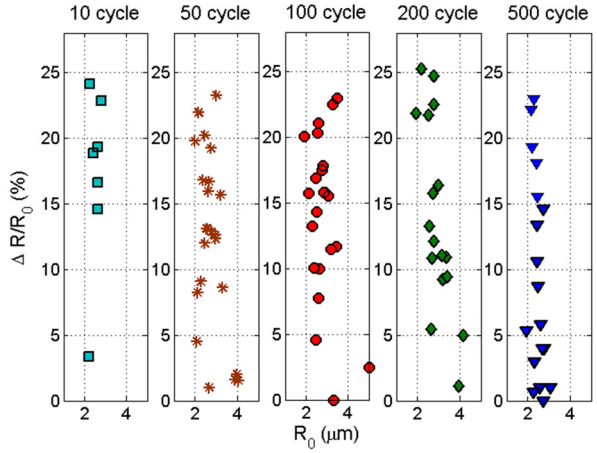

Figure 7. Acoustic dissolution as a function of acoustic cycles.

D. Static Dissolution

Static dissolution of MBs after ultrasound applications is strongly influenced by shell damage through insonation [5]. MBs shrinkage after ultrasound application was followed for 60 ms, and the radius change was plotted as a function of time in Figure 8 (A). We define the slope of the linear fitting for the plot as static dissolution coefficient, since it reflects the dissolution rate of MBs. The static dissolution coefficient is plotted in Figure 8(B). With increasing acoustically driven dissolution, the absolute value of static dissolution coefficient increases, indicating a correspondence between acoustic dissolution and loss of shell materials.

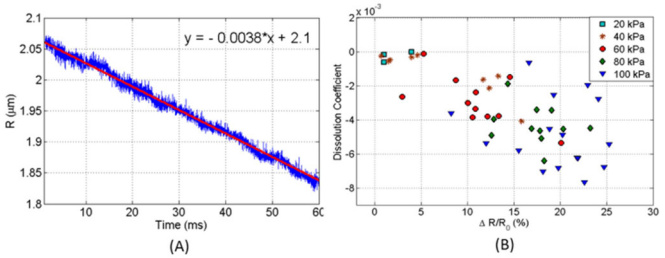

Figure 8. (A) Static dissolution of an individual microbubble within 60 ms after ultrasound application. (B) static dissolution coefficient as a function of acoustically driven dissolution.

IV. DISCUSSION

A. Release dynamics and drug-loading configurations

Borden and coworkers demonstrated a relation between the lipid composition on acoustic dissolution rate and proposed a mechanism of lipid shedding [7, 8]. They proposed that a less cohesive shell results in micron-scale or smaller particles of excess lipid material, while cohesive shells of loaded MBs can result in the buildup of shell-associated lipid strands and globular aggregates. Results from this study indicate that loaded bubbles show a higher occurrence of rearrangement as well as vesicle release, than unloaded bubbles. This can be explained by the previous work [7, 8], and our previous studies on loaded MBs, which show a higher shell viscosity than unloaded bubbles [6]. The less cohesive shell of unloaded bubbles leads to a higher occurrence of cloud release, while a more viscous shell of the loaded bubbles leads to a higher occurrence of release of the shell materials in clusters.

B. Release mechanisms

Acoustic dissolution during bubble compression is considered to be a key factor for shedding of the excessive shell materials [5], for unloaded microbubbles. Results from this study indicate a similar release mechanism for loaded MBs: acoustic dissolution leads to destruction of MBs shell, which in a further step causes corresponding static dissolution. For unloaded MBs, the released shell materials are clustered phospholipids that have formed a micelle or a bundle of lipid molecules. For loaded MBs, this can be clusters of liposomes that are detached, pulling parts of the lipids apart from the shell. In addition, results from this study showed a clear trend more on the dependence of acoustically driven dissolution on acoustical pressures rather than pulse length. This may indicate a major role of acoustic pressure on liposome release. However, this assumption needs further investigations.

C. Controlled drug delivery

High-speed fluorescence imaging provides detailed, time-resolved information about the ultrasound-triggered release of phospholipids and liposomes from MBs. It gives valuable insights into drug release dynamics and the ultrasound parameters required for controlled drug delivery. The release of shell materials from the bubble surface takes place at acoustic pressures as low as 20 kPa. It occurs at a time scale of microseconds and on a length scale of tens of microns. Both acoustical pressures and cycles play a role in controlling release dynamics, which also varies with different drug-loading configurations.

ACKNOWLEDGMENT

We would like to thank Frits Mastik, Robert Beurskens, Gert-Wim Bruggert and Martin Bos for their technical support. We also thank Guillaume Renaud and Tom Kokhuis for valuable discussions.

REFERENCES

[1] I. Lentacker, S. C. De Smedt, and N. N. Sanders, "Drug loaded microbubble design for ultrasound triggered delivery," Soft Matter, vol. 5, pp. 2161-2170, 2009.

[2] B. Geers, I. Lentacker, N. N. Sanders, J. Demeester, S. Meairs, and S. C. De Smedt, "Self-assembled liposome-loaded microbubbles: The missing link for safe and efficient ultrasound triggered drug-delivery," J Control Release, vol. 152, pp. 249-56, 2011.

[3] A. L. Klibanov, T. I. Shevchenko, B. I. Raju, R. Seip, and C. T. Chin, "Ultrasound-triggered release of materials entrapped in microbubble-liposome constructs: a tool for targeted drug delivery," J Control Release, vol. 148, pp. 13-7, 2010.

[4] E. C. Gelderblom, "Ultra-high-speed fluorescence imaging," Enschede, 2012.

[5] J. E. Chomas, P. Dayton, J. Allen, K. Morgan, and K. W. Ferrara, "Mechanisms of contrast agent destruction," IEEE Trans Ultrason Ferroelectr Freq Control, vol. 48, pp. 232-48, 2001.

[6] Y. Luan, T. Faez, Erik Gelderblom, I. Skachkov, B. Geers, I. Lentacker, T. van der Steen, M. Versluis, N. de Jong, "Acoustical properties of individual liposome-loaded microbubbles," Ultrasound in Medicine and Biology (accepted), 2012.

[7] M. A. Borden, D. E. Kruse, C. F. Caskey, S. K. Zhao, P. A. Dayton, and K. W. Ferrara, "Influence of lipid shell physicochemical properties on ultrasound-induced microbubble destruction," Ieee Transactions on Ultrasonics Ferroelectrics and Frequency Control, vol. 52, pp. 1992-2002, 2005.

[8] G. Pu, M. A. Borden, and M. L. Longo, "Collapse and shedding transitions in binary lipid monolayers coating microbubbles," Langmuir, vol. 22, pp. 2993-9, 2006.